Alkylborane Initiated RAFT Polymerization: Impact of Carboxylic Acid Deblockers

Olivia R. Wilson and Andrew J. D. Magenau*

Department of Materials Science and Engineering, Drexel University, Philadelphia, PA 19104, USA.

*Corresponding author: ajm496@drexel.edu

1. Reagents

The monomer (M), *N*, *N*-dimethylacrylamide (DMA, 99.5% stabilized with 100 ppm 4-methoxyphenol, Alfa Aesar) was used immediately after removal of the inhibitor by passage through a basic alumina column. The alkylborane-amine complex (R_3B-L), tri-*n*-butylborane methoxypropylamine, was donated by Callory LLC (Pittsburgh, PA) and stored in the glovebox until use. Propionic acid (PA, ≥ 99.1%, Sigma-Aldrich), formic acid (FA, 99%, Acros Organics), difluoroacetic acid (DFA, 98%, Thermo Scientific), and trifluoroacetic acid (TFA, > 99%, TCI Chemicals) were used as deblockers. The solvent used for all experiments was *N, N*-dimethylacetamide (DMac, > 99.5%, VWR). The internal standard for NMR was 1,3,5-trioxane (≥ 99%, Aldrich). 2,2,6,6-Tetramethylpiperidine 1-oxyl free radical (TEMPO, > 98%, TCI) was used as a radical quenching reagent. The chain transfer agents (CTA) were 2-doceylthiocarbonothioylthio)-2-methylpropionic acid (DDMAT, 98%, Sigma-Aldrich) and methyl 2-(dodecylthiocarbonothioylthio)-2-methylpropionate (MDMP, 97%, Sigma-Aldrich), which were used as received.

2. Equipment and Analytical Methods

2.1. Size Exclusion Chromatography (SEC): Relative number-average molecular weight (M_n), weight-average molecular weight, and polymer dispersity values were determined using SEC in *N,N*-dimethylacetamide. SEC analysis was conducted with a Shimadzu LC-20AD HPLC pump equipped with a Shimadzu RID-20A 120V refractive index detector using HPLC grade DMac containing 0.03 wt. % LiCl as the mobile phase. The polymer analytes were separated by two PLgel mixed-B Agilent columns connected in series at a flow rate of 1 mL/min and at 55°C. These columns were calibrated against 10 linear poly(methyl methacrylate) standards having M_n values between 800 and 2,570,000 g/mol.

2.2. Proton Nuclear Magnetic Resonance (^{1}H NMR): ^{1}H NMR was used to calculate monomer conversion. ^{1}H NMR spectra were obtained using a Varian Unity Inova-300 MHz or 500 MHz spectrometer at room temperature with deuterated chloroform ($CDCl_3$) as the NMR solvent. All spectra were recorded using 128 scans with a relaxation delay of 1 second. Trioxane was used as an internal standard for determining monomer conversion and all chemical shifts were referenced to chloroform.

3. Experimental Methods

3.1. AI-RAFT kinetic experiments: Kinetic experiments were performed at room temperature with PA as the deblocker and DDMAT as the CTA. A representative AI-RAFT kinetic procedure, formulated with 40 wt.% monomer and a molar ratio of [M]/[CTA]/[R_3B-L]/[D] ≈ 400/1/1/60, was conducted as follows. To a 20 mL scintillation vial was added DMA monomer (2.174 g, 21.93 mmol), R_3B-L (0.015 g, 0.0549 mmol), CTA (DDMAT, 0.02 g, 0.0549 mmol), trioxane (0.06 g), and 1.34 g DMac. The contents of the vial were then vortexed for 15 min, or longer, until complete dissolution occurred. Once a homogenous solution was obtained, a magnetic stir bar was added. The scintillation vial was then sealed using a rubber septum and electrical tape, and sparged with nitrogen for 1 h. After sparging, the scintillation vial was transferred into the glovebox, and a time zero sample was withdrawn for ^{1}H NMR analysis. To commence polymerization, a solution of deblocker (0.243 g PA, 3.291 mmol) and dissolved oxygen in DMac, having no prior deoxygenation, was also transferred into the glovebox and injected into the scintillation vial via syringe. The injected solution volume was kept constant at 1.69 mL to maintain a consistent amount of O_2 (8.78E-3 mmol) between experiments. After injecting the deblocker solution, the vial was briefly swirled and then placed on a stir plate for the course of polymerization. At each time point, an aliquot 0.02 mL, was withdrawn from the

polymerization and quenched by injection into a DMac solution containing a 10-fold excess of TEMPO to R_3B-L to prevent any further polymerization. Polymerization samples were then immediately prepared for ^1H NMR to determine monomer conversion and SEC to determine polymer molecular weight and dispersity. All kinetic experiments were conducted in at least duplicate.

3.2. AI-RAFT extent of reaction experiments: A representative AI-RAFT kinetic procedure, formulated with 40 wt.% monomer and a molar ratio of [M]/[CTA]/[R_3B-L]/[D] ≈ 400/1/1/60, was conducted as follows. Extent of reaction experiments were performed at room temperature with MDMP as the CTA. To a 20 mL scintillation vial was added DMA monomer (1.094 g, 11.04 mmol), R_3B-L (0.007 g, 0.027 mmol), CTA (MDMP, 0.01 g, 0.027 mmol), trioxane (0.03 g), and 1.48 g DMac. The contents of the vial were then vortexed for 15 min, or longer, until complete dissolution occurred. Once a homogenous solution was obtained, a magnetic stir bar was added. The scintillation vial was then sealed using a rubber septum and electrical tape, and sparged with nitrogen for 1 h. After sparging, the scintillation vial was transferred into the glovebox, and a time zero sample was withdrawn for ^1H NMR analysis. To commence polymerization, a solution of deblocker (0.117 g PA, 1.585 mmol) and dissolved oxygen in DMac, having no prior deoxygenation, was also transferred into the glovebox and injected into the scintillation vial via syringe. The injected solution volume was kept constant at 0.81 mL to maintain a consistent amount of O_2 between experiments. After injecting the deblocker solution, the vial was briefly swirled and then placed on a stir plate for the course of polymerization. The reaction was conducted for 20 h, and subsequently quenched by injection of a DMac solution containing a 10-fold excess of TEMPO to R_3B-L to prevent any further polymerization. Polymerization samples were then immediately prepared for ^1H NMR to determine monomer conversion and SEC to determine polymer molecular weight and dispersity.

3.4. pKa calculations for carboxylic acid deblockers: The pKa of each deblocker was predicted using MarvinSketch Software. Microspecies distribution plots were generated as a function of pH for each deblocker shown in **Figure S6**. The pKa is defined at the pH where 50% of the acid is deprotonated.

3.5. Calculation of moles of O_2 in oxygenated deblocker solutions containing deblocker and *N,N*-dimethylacetamide (DMac): The moles of O_2 added to the reaction mixture were estimated using the following equation given by **Eq. S1**.

(S1) $$moles\ of\ O_2 = \chi_G * moles\ of\ DMac$$

Where χ_G is the solubility of O_2 in DMac at room temperature and atmospheric pressure, which has a value of 4.82E-4. [1] In a typical kinetic experiment, the deblocker solution contained 1.69 mL or 0.0182 mol of DMac. Therefore, the moles of O_2 in a typical AI-RAFT experiment is approximately 8.78E-6 mol. Thus, the molar ratio of O_2/R_3B-L can be estimated at 0.16, which was kept constant across all reactions. It is important to emphasize that this calculation provides only a crude estimate of O_2 and doesn't account for many factors including O_2 solubility changes from other reagents (monomer, deblocker, etc.) or the amount of oxygen residing in the reactors head space.

4. Mechanisms and Rate Equations

4.1 Association/dissociation equilibrium of the alkylborane-ligand complex

Lewis pairs involving organoboranes, including alkylborane-amines, are known to exist in equilibrium between their dissociated (uncoordinated) and associated (coordinated) states. [2-5] Thus, protonation of the amine ligand, and loss of its Lewis basicity, disassociates the alkylborane-amine complex and liberates free alkylborane according to the following equilibrium. The equilibrium is therefore defined by **Eq. S2** and the concentration of R_3B given by **Eq. S3**.

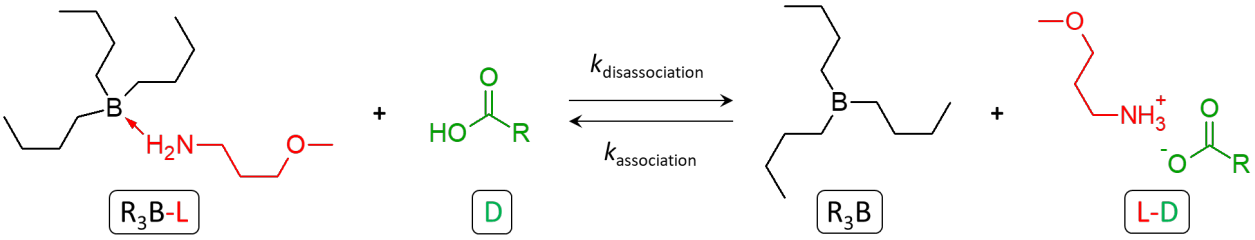

(S2) $$K_{eq} = \frac{k_{disassociation}}{k_{association}} = \frac{[R_3B][L-D]}{[R_3B-L][D]}$$

(S3) $$[R_3B] = \frac{[R_3B-L][D]K_{eq}}{[L-D]}$$

4.2 Autoxidation Mechanism 1 and Rate Equations

The first autoxidation mechanism of alkylboranes (AM1), adapted from literature, is provided below: [6-9]

Autoxidation Mechanism 1 (AM1)

1	R_3B	+	O_2	⟶	$R_2BOO•$	+	~~$R•$~~			
2	~~$R•$~~	+	O_2	⟶	~~$ROO•$~~					
3	~~$ROO•$~~	+	R_3B	⟶	R_2BOOR	+	$R•$			
overall	$2R_3B$	+	$2O_2$	$\xrightarrow{k_{AM1}}$	$R_2BOO•$	+	R_2BOOR	+	$R•$	

According to the above scheme, the rate of initiation (R_i) is:

(S4) $$R_i = \frac{d[P•]}{dt} = k_{AM1}[R_3B]^2[O_2]^2$$

The rate of bimolecular termination (R_t) in radical polymerization is given by:

(S5) $$R_t = -\frac{d[P•]}{dt} = k_t[P•]^2$$

Thus, under steady state conditions, $R_i = R_t$, and the concentration of propagating radicals ([P•]) is:

(S6) $$[P\bullet] = \sqrt{\frac{k_{AM1}[R_3B]^2[O_2]^2}{k_t}} = \left(\frac{k_{AM1}}{k_t}\right)^{1/2}[R_3B][O_2]$$

To relate the above expression to an alkylborane complex and a known quantity in the formulation of AI-RAFT, [R_3B] can be substituted for [R_3B-L] using **Eq. S3** to give the following expression:

(S7) $$[P\bullet] = \left(\frac{k_{AM1}}{k_t}\right)^{1/2}\left(\frac{[R_3B{-}L][D]K_{eq}}{[L{-}D]}\right)[O_2]$$

Thus, the overall rate of polymerization according to mechanism AM1 is:

(S8) $$R_p = -\frac{d[M]}{dt} = k_p[P\bullet][M] = k_p\left(\frac{k_{AM1}}{k_t}\right)^{1/2}\left(\frac{[R_3B{-}L][D]K_{eq}}{[L{-}DB]}\right)[O_2][M]$$

4.3 Autoxidation Mechanism 2 and Rate Equations

The second autoxidation mechanism, adapted from literature, is provided below: [10-13]

Autoxidation Mechanism 2 (AM2)

1 $\quad R_3B + O_2 \longrightarrow R_2BOOR$

2 $\quad R_2BOOR \longrightarrow R_2BO\bullet + RO\bullet$

overall $\quad R_3B + O_2 \xrightarrow{k_{AM2}} R_2BO\bullet + RO\bullet$

According to the above scheme, the rate of initiation (R_i) is:

(S9) $$R_i = \frac{d[P\bullet]}{dt} = k_{AM2}[R_3B][O_2]$$

The rate of bimolecular termination (R_t) in radical polymerization is given by:

(S10) $$R_t = -\frac{d[P\bullet]}{dt} = k_t[P\bullet]^2$$

Thus, under steady state conditions, $R_i = R_t$, and the concentration of propagating radicals ([P•]) is:

(S11) $$[P\bullet] = \sqrt{\frac{k_{AM2}[R_3B][O]_2}{k_t}} = \left(\frac{k_{AM2}}{k_t}\right)^{1/2}[R_3B]^{1/2}[O_2]^{1/2}$$

To relate the above expression to a known quantity and an alkylborane complex used in the formulation of AI-RAFT, [R_3B] can be substituted for [R_3B-L] using **Eq. 3** to give the following expression:

(S12) $$[P\bullet] = \left(\frac{k_{AM2}}{k_t}\right)^{1/2}\left(\frac{[R_3B{-}L][D]K_{eq}}{[L{-}D]}\right)^{1/2}[O_2]^{1/2}$$

Thus, the overall rate of polymerization according to mechanism AM2 is:

(S13) $$R_p = -\frac{d[M]}{dt} = k_p[P\bullet][M] = k_p\left(\frac{k_{AM2}}{k_t}\right)^{1/2}\left(\frac{[R_3B{-}L][DB]K_{eq}}{[L{-}DB]}\right)^{1/2}[O_2]^{1/2}[M]$$

5. Supplemental Figures and Tables

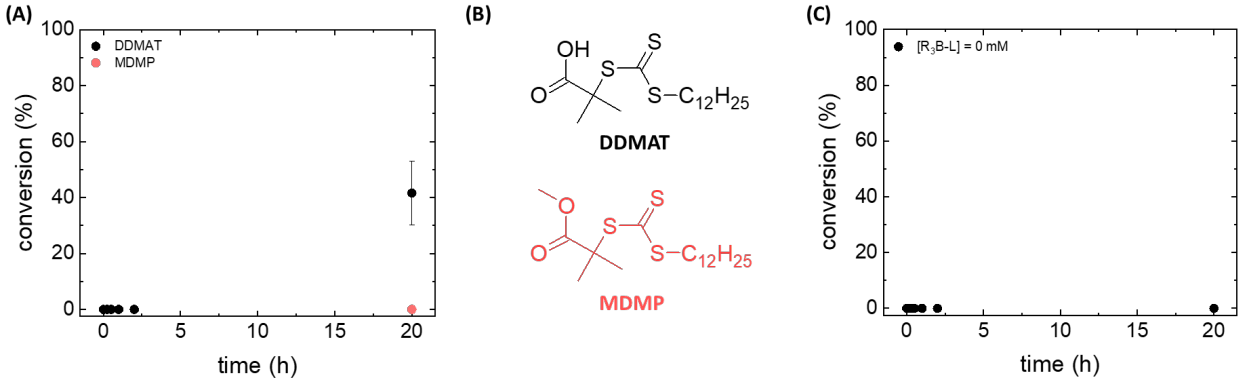

Figure S1: (A) Monomer conversion versus time without external added deblocker (no PA) using either DDMAT or MDMP as the CTA. Reaction conditions: [M]/[CTA]/[R_3B-L]/**[D]** ≈ 400/1/1/**0**, [M] ≈ 3.84 M or 40 wt.%. (B) Chemical structures of the CTAs. (C) Monomer conversion versus time for a control experiment without R_3B-L using DDMAT as the CTA and PA as the deblocker. Reaction conditions: [M]/[CTA]/**[R_3B-L]**/[D] ≈ 400/1/**0**/20, [M] ≈ 3.84 M or 40 wt.%.

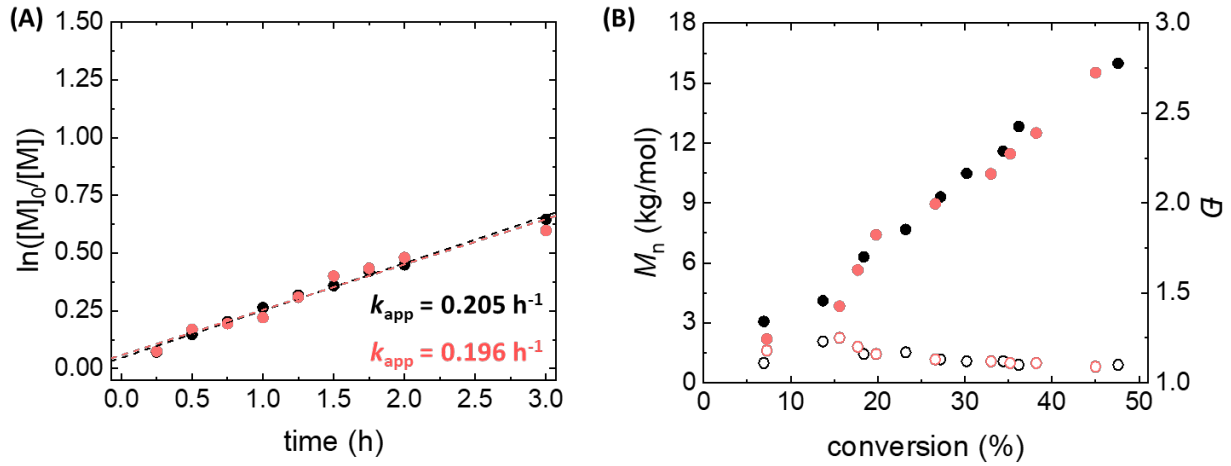

Figure S2: (A) First order kinetic plot and (B) molecular weight and dispersity versus conversion plot for [D] = [COOH] = 0.192 M. Reaction conditions: [M]/[CTA]/[R_3B-L]/**[D]** ≈ 400/1/1/**20**, [M] ≈ 3.84 M or 40 wt.%.

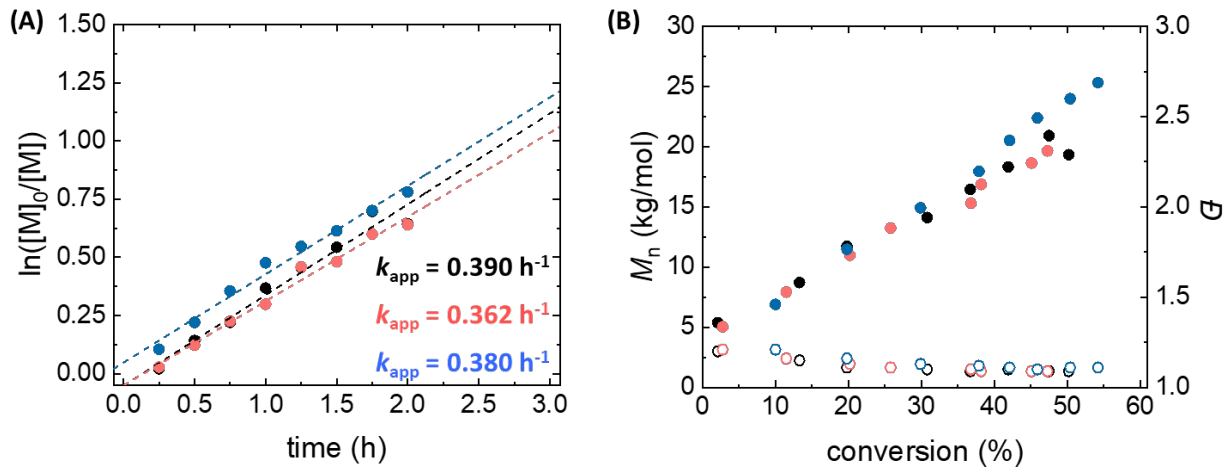

Figure S3: (A) First order kinetic plot and (B) molecular weight and dispersity versus conversion plot for [D] = [COOH] = 0.384 M. Reaction conditions: [M]/[CTA]/[R_3B-L]/**[D]** ≈ 400/1/1/**40**, [M] ≈ 3.84 M or 40 wt.%.

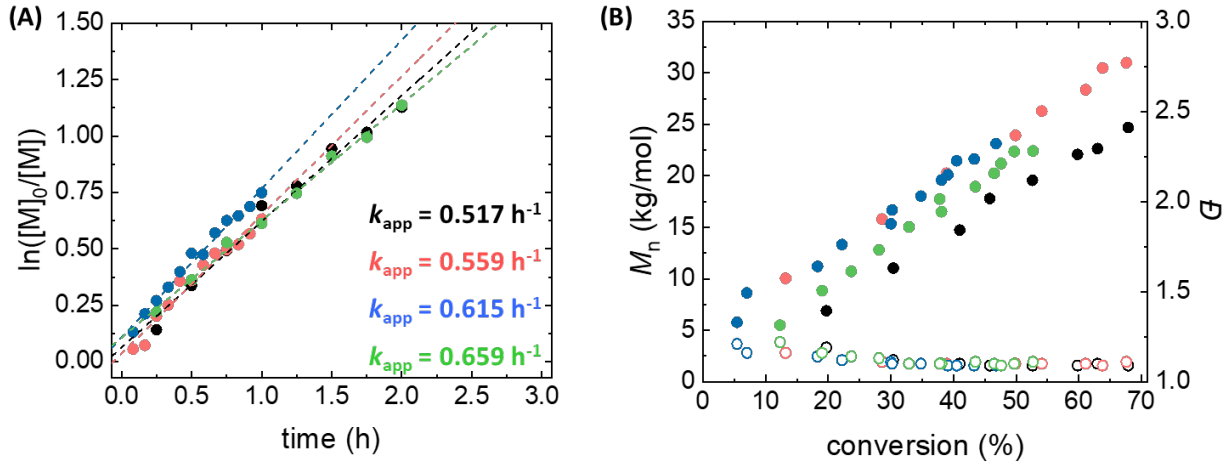

Figure S4: (A) First order kinetic plot and (B) molecular weight and dispersity versus conversion plot for [D] = [COOH] = 0.575 M. Reaction conditions: [M]/[CTA]/[R_3B-L]/**[D]** ≈ 400/1/1/**60**, [M] ≈ 3.84 M or 40 wt.%.

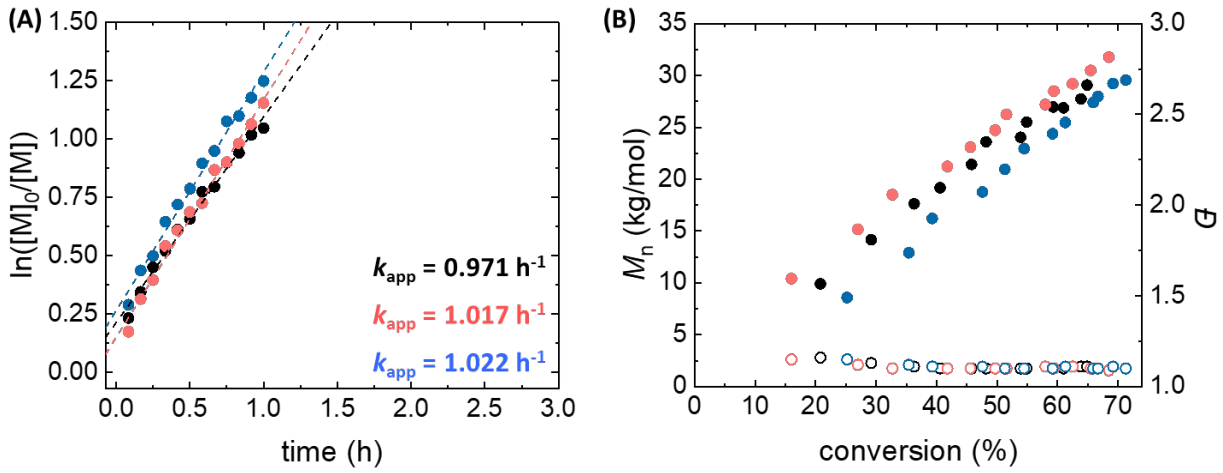

Figure S5: (A) First order kinetic plot and (B) molecular weight and dispersity versus conversion plot for [D] = [COOH] = 0.764 M. Reaction conditions: [M]/[CTA]/[R_3B-L]/**[D]** ≈ 400/1/1/**80**, [M] ≈ 3.84 M or 40 wt.%.

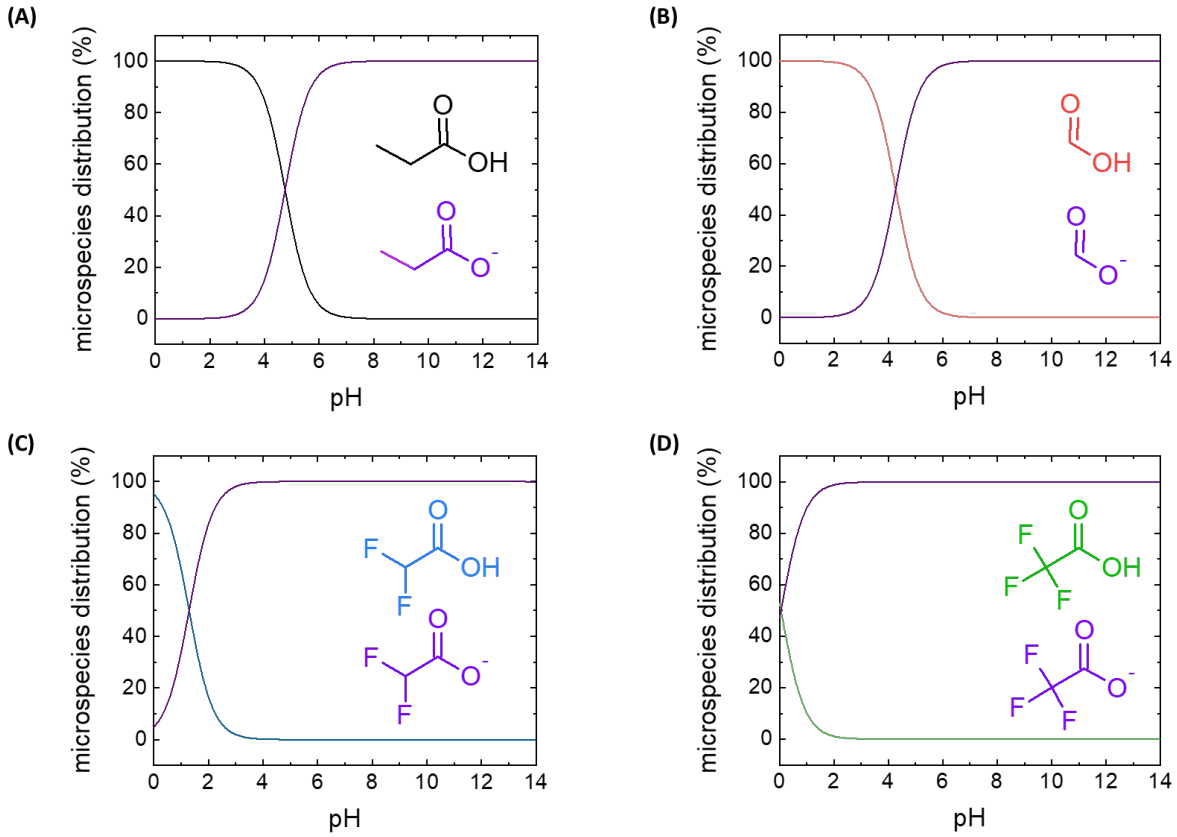

Figure S6: Microspecies distribution curves used to calculate the pKa for all deblockers. The pKa is the point when 50% of each acid species has been deprotonated: (A) propionic acid has pKa ~ 4.75, (B) formic acid has pKa ~ 4.27, (C) difluoroacetic acid has pKa ~ 1.30, and (D) trifluoroacetic acid has pKa ~ 0.05.

Table S1: Summary of AI-RAFT formulations and results with four different carboxylic acid deblockers.

Entry	Deblocker	[M]/[CTA]/[R_3B-L]/[D]				[D]/[R_3B-L]	Conversion (%)	M_n (g/mol)	M_n, theo (g/mol)	$Đ$
1	PA	364	1	0.90	0.25	0.25	0	N/A	N/A	N/A
2	PA	364	1	0.90	0.46	0.52	0	N/A	N/A	N/A
3	PA	366	1	0.90	0.89	1.00	0	N/A	N/A	N/A
4	PA	400	1	1	5.00	4.81	18.5	5,826	7,033	1.18
5	PA	364	1	0.90	9.20	10.4	23.1	7,910	8,364	1.16
6	PA	400	1	0.98	20.4	20.9	52.6	25,040	20,775	1.09
7	PA	363	1	0.95	37.3	39.3	82.2	32,879	29,684	1.11
8	PA	369	1	0.97	54.6	56.5	89.6	35,310	32.898	1.11
9	PA	406	1	0.98	82.1	84.0	88.5	33,558	35,507	1.10
10	FA	370	1	1.02	0.26	0.25	0	N/A	N/A	N/A
11	FA	364	1	0.95	0.45	0.47	0	N/A	N/A	N/A
12	FA	406	1	1.12	1.07	0.95	29.3	6,905	11,786	1.18
13	FA	366	1	0.90	5.23	5.89	67.6	26,089	24,411	1.11
14	FA	405	1	1.12	12.7	11.3	82.3	32,890	33,017	1.13
15	FA	367	1	0.89	20.1	22.7	75.7	29,849	27,432	1.13
16	FA	366	1	0.90	36.5	41.1	76.4	30,702	27,757	1.12
17	FA	366	1	0.90	55.5	62.4	72.9	26,375	26,553	1.09
18	FA	368	1	0.90	73.4	82.6	71.3	26,744	25,992	1.10
19	DFA	400	1	1.08	0.25	0.23	0	N/A	N/A	N/A
20	DFA	404	1	1.08	0.49	0.45	64.5	29,312	25,770	1.11
21	DFA	400	1	1.08	1.00	0.97	96.2	34,662	38,435	1.18
22	DFA	400	1	1.08	5.00	4.85	83.2	32,774	33,241	1.15
23	DFA	400	1	1.08	10.0	9.81	73.8	28,733	29,485	1.12
24	DFA	364	1	0.90	19.1	21.5	71.4	28,285	25,851	1.14
25	DFA	363	1	1.02	36.5	36.0	78.8	33,284	28,382	1.17
26	DFA	404	1	0.98	60.7	62.1	80.4	31,757	32,341	1.15
27	DFA	401	1	0.98	81.2	83.0	71.4	30,701	28,274	1.14
29	TFA	400	1	0.98	0.28	0.29	0	N/A	N/A	N/A
30	TFA	406	1	0.98	0.55	0.56	72.8	29,682	29,284	1.12
31	TFA	416	1	1.12	1.09	0.97	75.8	29,745	31,201	1.12
32	TFA	406	1	1.05	5.62	5.36	73.8	31,021	29,669	1.16
33	TFA	369	1	0.91	9.16	10.0	63.5	24,677	23,272	1.11
34	TFA	366	1	1.02	18.7	18.3	69.0	25,175	24,982	1.11
35	TFA	400	1	1	40.0	38.4	61.5	24,189	23,380	1.11
36	TFA	400	1	1	60.0	57.7	74.3	26,397	28,246	1.12
37	TFA	400	1	1	80.0	76.9	65.8	26,890	25,015	1.12

a: Each entry represents an individual polymerization. All polymerizations were conducted at room temperature for 20 h using 40 wt. % monomer in DMac. Polymerizations were initiated using 0.81 mL of DMac solutions of deblocker without deoxygenation.

b: Monomer conversion was calculated using ^{1}H NMR with a trioxane internal standard.

c: Theoretical molecular weight was determined as, $M_{n,theo.} = MW_{monomer} \cdot ([DMA]/[CTA]) \cdot conversion + MW_{CTA}$.

Supporting Information References:

[1] Sato, T.; Hamada, Y.; Sumikawa, M.; Araki, S.; Yamamoto, H. Solubility of Oxygen in Organic Solvents and Calculation of the Hansen Solubility Parameters of Oxygen. *Ind. Eng. Chem. Res.* **2014**, 53, 19331. https://doi.org/10.1021/ie502386t

[2] Brown, H. C. Studies in Stereochemistry. V. The Effect of F-Strain on the Relative Base Strengths of Ammonia and Trimethylamine. *J. Am. Chem. Soc.* **1945**, 67, 374. https://doi.org/10.1021/ja01219a007

[3] Brown, H. C. Studies in Stereochemistry. VI. The Effect of F-Strain on the Relative Base Strengths of Ammonia and the Methylamines. *J. Am. Chem. Soc.* **1945**, 67, 378. https://doi.org/10.1021/ja01219a008

[4] Vidal, F.; Gomezcoello, J.; Lalancette, R. A.; Jäkle, F. Lewis Pairs as Highly Tunable Dynamic Cross-Links in Transient Polymer Networks. *J. Am. Chem. Soc.* **2019**, 141, 15963. https://doi.org/10.1021/jacs.9b07452

[5] Povie, G.; Marzorati, M.; Bigler, P.; Renaud, P. Role of Equilibrium Associations on the Hydrogen Atom Transfer from the Triethylborane–Methanol Complex. *Journal of Organic Chemistry* **2013**, 78, 1553. https://doi.org/10.1021/jo302576c

[6] Brown, H. C.; Midland, M. M. Initiation rates for autoxidation of trialkylboranes. Effect of a steric factor on the initiation rate. *J. Chem. Soc. D: Chem. Comm.* **1971**, 699. https://doi.org/10.1039/C29710000699

[7] Ollivier, C.; Renaud, P. Organoboranes as a Source of Radicals. *Chem. Rev.* **2001**, 101, 3415. https://doi.org/10.1021/cr010001p

[8] Renaud, P.; Beauseigneur, A.; Brecht-Forster, A.; Becattini, B.; Darmency, V.; Kandhasamy, S.; Montermini, F.; Ollivier, C.; Panchaud, P.; Pozzi, D.; Scanlan Eoin, M.; Schaffner, A.-P.; Weber, V., Boron: A key element in radical reactions. *Pure Appl. Chem.*, **2007**; 79, 223. https://doi.org/10.1351/pac200779020223

[9] Alagi, P.; Hadjichristidis, N.; Gnanou, Y.; Feng, X. Fast and Complete Neutralization of Thiocarbonylthio Compounds Using Trialkylborane and Oxygen: Application to Their Removal from RAFT-Synthesized Polymers. *ACS Macro Lett.* **2019**, 8, 664. https://doi.org/10.1021/acsmacrolett.9b00357

[10] Welch, F. J. Polymerization of Methyl Methacrylate by Triethylboron–Oxygen Mixtures. *J. Polym. Sci.* **1962**, 61, 243. https://doi.org/10.1002/pol.1962.1206117125

[11] Sonnenschein, M. F.; Webb, S. P.; Kastl, P. E.; Arriola, D. J.; Wendt, B. L.; Harrington, D. R.; Rondan, N. G. Mechanism of Trialkylborane Promoted Adhesion to Low Surface Energy Plastics. *Macromolecules* **2004**, 37, 7974. https://doi.org/10.1021/ma040095f

[12] Sonnenschein, M. F.; Webb, S. P.; Redwine, O. D.; Wendt, B. L.; Rondan, N. G. Physical and Chemical Probes of the Bond Strength between Trialkylboranes and Amines and Their Utility as Stabilized Free Radical Polymerization Catalysts. *Macromolecules* **2006**, 39, 2507. https://doi.org/10.1021/ma060268w

[13] Ahn, D.; Wier, K. A.; Mitchell, T. P.; Olney, P. A. Applications of Fast, Facile, Radiation-Free Radical Polymerization Techniques Enabled by Room Temperature Alkylborane Chemistry. *ACS Appl. Mater. Interfaces* **2015**, 7, 23902. https://doi.org/10.1021/acsami.5b05943